

# A modified Susceptible-Infected-Recovered model for observed under-reported incidence data

Imelda Trejo<sup>1,2\*</sup>, Nicolas Hengartner<sup>1,2†</sup>

**1** Theoretical Biology and Biophysics Group, Los Alamos National Laboratory, Los Alamos, Nuevo Mexico, United States of America

✉These authors contributed equally to this work.

†Senior authorship.

\* imelda@lanl.gov

## Abstract

Fitting Susceptible-Infected-Recovered (SIR) models to incidence data is problematic when a fraction  $q$  of the infected individuals are not reported. Assuming an underlying SIR model with general but known distribution for the time to recovery, this paper derives the implied differential-integral equations for observed incidence data when a fixed fraction  $q$  of newly infected individuals are not observed. The parameters of the resulting system of differential equations are identifiable. Using these differential equations, we develop a stochastic model for the conditional distribution of current disease incidence given the entire past history of incidences. This results in an epidemic model that can track complex epidemic dynamics, such as outbreaks with multiple waves. We propose to estimate of model parameters using Bayesian Monte-Carlo Markov Chain sampling of the posterior distribution. We apply our model to estimate the infection rate and fraction of asymptomatic individuals for the current Coronavirus 2019 outbreak in eight countries in North and South America. Our analysis reveals that consistently, about 70-90% of infected individuals were not observed in the American outbreaks.

## Author summary

Quantifying the lethality and infectiousness of emerging diseases such as the coronavirus disease (COVID-19) pandemic is challenging because of under-reporting of incidence cases. Under-reporting can be attributed to the presence of sub-clinical infections, asymptomatic individuals and lack of systematic testing. We develop an extension of standard epidemiological models to describe the temporal observed dynamics of infectious diseases and to estimate the under-reporting from incidence data. The extended model shows that fitting SIR model types directly to incidence data will under-estimate the true infectiousness of the disease. Therefore, failing to account for the under-reporting will under-estimate the severity of the outbreak, possibly leading decision makers to call the epidemic under control prematurely. Additionally, from the extended model formulation, we present a novel stochastic framework to approximate daily infectious incidence cases given the past observed cases and to propose a likelihood function for the model parameters: the infection rate and fraction of under-reporting cases. By using the COVID-19 time series of newly reported incidence cases from the World Health Organization for various American countries, we show the functionality of

the model to estimate transmission parameters and track the various complex evolving epidemic trajectories.

## 1 Introduction

Susceptible-Infected-Recovered (SIR) models, introduced by Kermack and McKendrick and further developed by Wilson and Worcester [1, 2], have been extensively used to describe the temporal dynamic of infectious disease outbreaks [3–5]. They have also been widely used to estimate the disease infection rate by fitting the models to observed incidence data [6–8], such as time series of daily or weekly reported number of new cases provided by [9–12], for example. Implicit in all these model fitting is the assumption that all the infected individuals are observed. Yet that assumption is problematic when disease incidences are under-reported. Under-reporting of incidence is prevalent in health surveillance of emerging diseases [13, 14], and also occurs when a disease presents a large fraction of asymptomatic carriers, e.g., Typhoid fever, hepatitis B, Epstein-Barr virus [15] and Zika [16]. Lack of systematic testing and the presence of sub-clinical patients, which are prevalent in both Severe acute respiratory syndrome coronavirus 2 (SARS-CoV-2), the cause of the coronavirus disease (COVID-19) pandemic [17–20], and Influenza [21, 22], also leads to under-counting incidence and death. Fitting directly a SIR to raw under-reported incidence counts will underestimate the infection rate (see Section 2.2.2), and therefore failing to account for the under-reporting will under-estimate the severity of the outbreak, possibly leading decision makers to call the epidemic under control prematurely.

To account for under-reporting in a SIR model type, Shutt *et. al* [23] propose to split the infected individuals into two: an observed category and an unobserved category. This is a special case of the Distributed Infection (DI) models introduced in [24]. However, fitting this model to data is problematic since there are no data from the unobserved category. Furthermore, making inference about DI model parameters is difficult as there are no adequate stochastic model extensions for the DI models, which implies that there is no analytic expression for the likelihood. A partial solution of this problem is to use Approximate Bayesian Computations as in [23] or relies on particle filtering [25]. Finally, we mention two recent approaches to model asymptomatic individuals in SIR-type models: First Lopman *et. al.* in [26] model Norovirus outbreaks using an SEIR model where the infected would progress from symptomatic to asymptomatic to immune. Once immune, individuals can cycle between immune and asymptomatic infection. Second Kalajdzievska *et. al.* in [15] propose an SIcIR model where infected individuals are separated into asymptomatic and symptomatic groups by a given probability as they progress from the susceptible group.

The aim of this paper is to present a novel approach to estimate the under-reporting from daily incidence data and apply this methodology to estimate the under-reporting of COVID-19 data. COVID-19 pandemic is a particular example of infectious diseases that poses many of the challenges to quantify the newly incidence cases, and hence to estimate its infectiousness [19, 27, 28], as under-reporting arises from the presence of sub-clinical infections [20, 29], asymptomatic individuals [30, 31], and lack of systematic testing [17, 18]. Accordingly, asymptomatic individuals account for 20–70% of all the infections [30]. Additionally, early in China outbreak, before traveling restrictions, 86% of all infections were not documented [19].

In the development of our methodology, we present two innovations: First, we introduce an alternative to the DI models that directly describes the dynamic of the observed under-reported incidences. Specifically, assuming that a constant fraction  $p < 1$  of the newly infected individuals are observed, we derive a set of integral-differential equations describing the temporal dynamic of the observed number

of observed incidence. Second, we use the local dynamic of the observed incidence to propose a model for the conditional expectation of new cases given the past observed history. Making additional distributional assumptions, we obtain a likelihood for the model parameters: the infection rate  $\beta$  and the fraction  $p$  of observed incidence. We refer to Bettencourt and Ribeiro [32] for an interesting alternative framework that leads to a likelihood for the basic reproduction number  $\mathcal{R}_0$ . We show that as the epidemic progresses, both of these parameters become identifiable.

## 2 Materials and methods

### 2.1 Data source

The time series of daily number of confirmed COVID-19 cases and total population,  $N$ , for each country were obtained from the World Health Organization (WHO) reports, from January 03 to November 10, 2020. Both data sets are freely available online [12, 33].

### 2.2 Model development

The model is developed in three steps. First, we present a generalized SIR epidemic model formulation, which is then extended to model the dynamic of the observed evolving infection. Second, we introduce a stochastic model to quantify the conditional expectation of newly incidence cases given the past time series of observed incidence counts. Third, we propose a methodology to approximate the conditional expectation of the newly incidence cases, which can be easily implemented in programming languages.

#### 2.2.1 Generalized SIR model

Classical mass-action epidemic models, such as the SIR models are simple yet useful mathematical descriptions of the temporal dynamics of disease outbreak [3–5]. These models describe the temporal evolution of the number of susceptible  $S(t)$ , infected  $I(t)$  and recovered  $R(t)$  individuals in a population of fixed size  $N = S(t) + I(t) + R(t)$ . We model their dynamic through the set of integral-differential equations [34]:

$$S'(t) = -\frac{\beta}{N}S(t)I(t) \quad (1)$$

$$I(t) = \int_0^t (-S'(u))(1 - F(t-u))du + I_0(1 - F(t)) \quad (2)$$

$$R(t) = \int_0^t (-S'(u))F(t-u)du + R_0 + I_0F(t), \quad (3)$$

with initial conditions  $S_0, I_0, R_0$ . The parameter  $\beta$  measures the infection rate and the function  $F(t)$  is the cumulative distribution of the time from infection to recovery. When  $F(t) = 1 - e^{-\gamma t}$  is the exponential distribution with mean  $\gamma^{-1}$ , our model reduces to the standard SIR model, see Murray [35, Chapter 19] for example. For completeness of this work, the proof of existence and unique solution of System (1,2,3) is provided in the appendix, an alternative prove can be found in [34].

The model parameters  $\beta$  and  $F(t)$  are epidemiologically relevant and provide insights into the outbreak. For example, the basic reproductive number as defined by Lotka [36, 37]:

$$\mathcal{R}_0 = \int_0^\infty \frac{\beta}{N}S(t)(1 - F(t))dt \approx \frac{\beta}{\gamma}, \quad (4)$$

where  $\gamma^{-1} = \int_0^\infty (1 - F(t))dt$  is the average recovery time, is arguably the most widely used measure of the severity of an outbreak [38, 39], at least in the absence of interventions to control it. It measures the expected number of secondary infections attributed to the index case in a naïve population. Other quantities of interest, such as the maximum number of infected individuals and the total number of infections can be expressed in terms of the reproductive number  $\mathcal{R}_0$ , e.g. Weiss [40].

For many diseases, it is reasonable to assume that the disease progression, from infection to recovery, is known, either because the disease is well characterized or because date of onset of symptoms, hospital admission and discharge data are available [41]. Thus we will assume throughout this paper that we know the distribution of the recovery period  $F(t)$  and we focus on estimating the infection rate  $\beta$ .

### 2.2.2 Modeling the number of observed disease incidence

Let  $\tilde{S}(t)$ ,  $\tilde{I}(t)$  and  $\tilde{R}(t)$  denote the observed number of susceptible, infected and recovered individuals as a function of time. We make the following modeling assumptions:

- (A1) The true underlying dynamic follows a SIR described by Eqs (1) to (3) with known fixed population size  $N$  and time to recovery distribution  $F(t)$ .
- (A2) A constant fraction  $p$  of newly infected individuals are observed. That is  $\tilde{S}'(t) = pS'(t)$ . The same fraction  $p$  of initial cases are observed, i.e.,  $\tilde{I}_0 = pI_0$ ,  $\tilde{R}_0 = pR_0$ , and  $\tilde{S}_0 = N - \tilde{I}_0 - \tilde{R}_0$ .
- (A3) The recovery distribution is the same for the observed and unobserved infected individuals.

Under these assumptions, the observed number of infected individuals at time  $t$  is

$$\tilde{I}(t) = \int_0^t \left( -\tilde{S}'(u) \right) (1 - F(t - u)) du + \tilde{I}_0 (1 - F(t)) = p \cdot I(t), \quad (5)$$

and similarly,  $\tilde{R}(t) = p \cdot R(t)$ . The number of “observed” susceptible individuals is

$$\tilde{S}(t) = (1 - p)N + pS(t). \quad (6)$$

Eq (6) follows by solving the differential equation  $\tilde{S}'(t) = pS'(t)$  and using the identity  $\tilde{S}_0 = N(1 - p) + pS_0$ , which results from the hypotheses (A2) and  $N = S_0 + I_0 + R_0$ . These equations capture the intuitive idea that under-reported incidence results in a larger number of observed susceptible and fewer infected and recovered individuals through the epidemic evolution.

Consider the ratio, which yields from Assumption (A2) and Eqs (5) and (6):

$$\frac{-\tilde{S}'(t)}{\tilde{S}(t)\tilde{I}(t)} = \frac{-pS'(t)}{pI(t) [(1 - p)N + pS(t)]} = \frac{\beta}{N} \cdot \frac{S(t)}{(1 - p)N + pS(t)} = \frac{\beta}{N} \cdot v(t). \quad (7)$$

For a standard SIR model with  $p = 1$ , that ratio  $v(t)$  is unity. However, for the observed process, the ratio  $v(t)$  starts at one and then monotonically decreases over time. It follows that fitting an SIR model to observed incidence data, neglecting the under-reporting, will produce a nearly unbiased, but possibly noisy estimate for  $\beta$  early in the outbreak when  $v(t) \approx 1$ . As more data becomes available and  $v(t)$  decreases, the estimated infection rate  $\beta$  will under-estimate the true value. As a consequence, one might at later times in an outbreak, under-estimate the severity of the outbreak and call the epidemic under control prematurely.

The relationship between the actual and observed quantities are used to describe the temporal dynamic of the observed number of incidence.

**Theorem 1** Under assumptions (A1), (A2), and (A3), the process of the observed individuals evolves according to the following set of integral-differential equations:

$$\tilde{S}'(t) = -\frac{\beta}{Np} \tilde{S}(t) \tilde{I}(t) + \frac{\beta(1-p)}{p} \tilde{I}(t) \quad (8)$$

$$\tilde{I}(t) = \int_0^t \left( -\tilde{S}'(u) \right) (1 - F(t-u)) du + \tilde{I}_0 (1 - F(t)) \quad (9)$$

$$\tilde{R}(t) = \int_0^t \left( -\tilde{S}'(u) \right) F(t-u) du + \tilde{R}_0 + \tilde{I}_0 F(t). \quad (10)$$

The conclusion of the theorem follows from algebraic manipulations of Eqs (1) to (6). The addition of the positive term  $((1-p)\beta/p)\tilde{I}(t)$  to  $\tilde{S}'(t)$  leads to a slower depletion rate of the observed susceptible population than would be expected under a SIR model.

### 2.2.3 A stochastic model for the observed incidence

Observed incidence of disease are typically reported at regular time interval. Precisely, let  $0 = t_0 < t_1 < t_2 < \dots < t_n$  denote the boundary of the observation window. For simplicity, we assume that  $t_k = k\Delta$ , and we denote by  $Y_k$  the number of new cases observed in the interval  $(t_{k-1}, t_k]$ ,  $k = 1, 2, \dots, n$ . Our model for new incidences  $Y_k$  will depend on the actual observed past history of incidences  $\mathcal{H}_{k-1} = \{Y_1, Y_2, \dots, Y_{k-1}\}$ . As a result, our model will take into account stochastic fluctuations in incidences. Indeed, imagine that the reported incidences  $Y_j$  is much larger than what is predicted by Model (8,9,10). That excess of cases will alter the observed dynamic of the outbreak, making it progress faster. Similarly, smaller number of incidences will slow down the outbreak. Therefore, taking into account these effects, we first model locally the dynamic of the process at each time interval given the history and then we model the conditional expectation of new cases occurring in the interval.

Let  $\tilde{S}_k(t)$  and  $\tilde{I}_k(t)$  denote the temporal variables of the epidemic process observed in the interval  $(t_{k-1}, t_k]$ . Then, from Eqs (8) and (9):

$$\tilde{S}'_k(t) = -\frac{\beta}{Np} \tilde{S}_k(t) \tilde{I}_k(t) + \frac{\beta(1-p)}{p} \tilde{I}_k(t) \quad (11)$$

$$\begin{aligned} \tilde{I}_k(t) &= \int_{t_{k-1}}^t \left( -\tilde{S}'_k(u) \right) (1 - F(t-u)) du + \sum_{j=1}^{k-1} \int_{t_{j-1}}^{t_j} \left( -\tilde{S}'_j(u) \right) (1 - F(t-u)) du \\ &+ \tilde{I}_0 (1 - F(t)), \end{aligned} \quad (12)$$

for all  $t_{k-1} < t \leq t_k$ . Additionally, from hypothesis, the initial condition  $\tilde{S}_{k-1} = \tilde{S}_k(t_{k-1})$  is given by

$$\tilde{S}_{k-1} = \tilde{S}_0 - \sum_{j=1}^{k-1} Y_j, \quad (13)$$

with the convention  $\sum_{j=1}^0 Y_j = 0$ . Eq (12) follows directly from Eq (9) by partitioned the time line into the observed intervals and using the definition of each  $\tilde{S}_j(t)$  variable. Hence, System (11,12,13) models the local epidemic dynamics in the interval  $(t_{k-1}, t_k]$  and it is linked with the time series of observed incidences through Eq (13) and

$$\int_{t_{j-1}}^{t_j} \left( -\tilde{S}'_j(u) \right) du = Y_j, \quad (14)$$

for all  $j = 1, 2, \dots, k-1$ .

From the local dynamics, Eqs (11) to (13), the calculation of  $Y_k$  depends on the full history of the susceptible and infected  $\tilde{S}_0, \tilde{S}_1(t), \dots, \tilde{S}_{k-1}(t), \tilde{I}_0, \tilde{I}_1(t), \dots, \tilde{I}_{k-1}(t)$  individuals, i.e.,

$$Y_k = \mathbb{E}[Y_k | \tilde{S}_0, \tilde{S}_1(t), \dots, \tilde{S}_{k-1}(t), \tilde{I}_0, \tilde{I}_1(t), \dots, \tilde{I}_{k-1}(t)] \quad (15)$$

$$= \int_{t_{k-1}}^{t_k} \frac{\beta}{Np} \tilde{S}_k(u) \tilde{I}_k(u) - \frac{\beta(1-p)}{p} \tilde{I}_k(u) du. \quad (16)$$

We propose to approximate  $Y_k$  such that the approximation depends only on the time series,  $Y_1, \dots, Y_{k-1}$ , by further assuming that the incidence cases are uniformly distributed in their observational window and using Eq (12) to posit the following definition.

**Definition 1** Let  $Y_1, Y_2, \dots, Y_k$  the sequence of observed incidence. We model their conditional expectation as

$$\mu_k = \mathbb{E}[Y_k | Y_1, \dots, Y_{k-1}] = \int_{t_{k-1}}^{t_k} \frac{\beta}{Np} \tilde{S}_k(u) \tilde{I}_k(u) - \frac{\beta(1-p)}{p} \tilde{I}_k(u) du, \quad (17)$$

where  $\tilde{S}_k(u)$  and  $\tilde{S}_{k-1}$  satisfy Eqs (11) and (13), respectively, and

$$\tilde{I}_k(t) = \int_{t_{k-1}}^t (-\tilde{S}'_k(u)) (1 - F(t-u)) du + \sum_{j=1}^{k-1} \frac{Y_j}{\Delta} \int_{t_{j-1}}^{t_j} (1 - F(t-u)) du + \tilde{I}_0 (1 - F(t)) \quad (18)$$

for all  $t_{k-1} < t \leq t_k$ .

From Definition 1, given  $\mu_k$  we model the conditional distributions of  $Y_k$  given  $\mathcal{H}_{k-1}$  with a negative binomial distribution, i.e.,

$$Y_k | Y_1, \dots, Y_{k-1} \sim \text{NegBinom} \left( \frac{\mu_k}{\mu_k + r}, r \right). \quad (19)$$

With this parametrization, the expected and variance values are

$$\mathbb{E}[Y_k] = \mu_k \quad \text{and} \quad \mathbb{V}[Y_k] = \mathbb{E}[Y_k] + \frac{\mu_k^2}{r}, \quad (20)$$

in which the parameter  $r$  controls the amount of over dispersion. As the over dispersion increases with the mean, and  $r$  very large makes the model more similar to a Poisson distribution. Therefore, the advantage of the negative binomial over the Poisson, is that it accounts for over dispersion, which we expect since we have averaged away the stochasticity of the recoveries. Other distributions are possible, such as beta negative binomial distribution [42] or the Conway-Maxwell-Poisson distribution [43].

Using the negative binomial distribution assumption, we are now able to write down an approximate likelihood for the infection rate and the fraction of new observed cases. Given a time series  $\mathcal{H}_{k-1}$ , the likelihood for  $\beta$  and  $p$  with  $r$  fixed is

$$L(\beta, p) = \prod_{k=2}^n \mathbb{P}[Y_k | Y_1, \dots, Y_{k-1}] \times \mathbb{P}[Y_1] \quad (21)$$

$$\propto \prod_{k=2}^n \frac{\mu_k^{y_k} (\beta, p)}{(\mu_k (\beta, p) + r)^{y_k + r}} \times \mathbb{P}[Y_1], \quad (22)$$

where  $\mu_k = \mu_k^{y_k} (\beta, p)$  emphasizes its dependence on the model parameters. Since in the model formulation, the distribution of  $Y_1$  does not contain any information about the

infection rate and the fraction of observed cases, the term  $\mathbb{P}[Y_1]$  is dropped from the likelihood. Resulting the equation

$$l(\beta, p) = \sum_{k=2}^n y_k \log(\mu_k(\beta, p)) - (r + y_k) \log(\mu_k(\beta, p) + r) \quad (23)$$

as an estimator for the natural logarithm of  $L(\beta, p)$ .

#### 2.2.4 Approximation of the conditional expectation

To reduce the computational burden of having to solve numerically Eq (17), we propose to estimate the conditional expectation  $\mu_k$  by linearizing both  $\tilde{S}_k(u)$  and  $\tilde{I}_k(u)$  around  $t_{k-1}$  in the integrand of this equation and solve it. The below lemma summarizes the resulting approximation, whose proof is provided in the appendix.

**Lemma 1** *Let us assume that each observed incidence  $Y_1, Y_2, \dots, Y_{k-1}$  is uniformly distributed in its observed interval, i.e.,*

$$-S'_j(u) = Y_j/\Delta, \quad \text{for all } u \in (t_{j-1}, t_j] \quad (24)$$

and  $j = 1, \dots, k-1$ . Then the conditional expectation  $\mu_k$  can be approximated with

$$\mu_k = -\Delta \tilde{S}'_{k-1} \left[ 1 + \frac{\Delta}{2} \left( \frac{\tilde{I}'_{k-1}}{\tilde{I}_{k-1}} - \frac{\beta}{p} \frac{\tilde{I}_{k-1}}{N} \right) - \frac{\beta \Delta^2}{3p} \frac{\tilde{I}'_{k-1}}{N} \right] \quad (25)$$

when  $\tilde{I}_{k-1} \neq 0$  and  $(\tilde{I}_0 + \tilde{R}_0 + \sum_{j=1}^{k-1} Y_j)/N \leq p < 1$  or  $\mu_k = 0$  otherwise. The values  $\tilde{S}'_{k-1}$ ,  $\tilde{I}'_{k-1}$ , and  $\tilde{I}_{k-1}$  are defined as

$$\tilde{S}'_{k-1} = -\frac{\beta}{p} \left[ \frac{\tilde{S}_{k-1}}{N} - (1-p) \right] \tilde{I}_{k-1} \quad (26)$$

$$\tilde{I}'_{k-1} = -\sum_{j=1}^{k-1} \frac{Y_j}{\Delta} [F(\Delta(k-j)) - F(\Delta(k-j-1))] - \tilde{S}'_{k-1} - \tilde{I}_0 f(t_{k-1}) \quad (27)$$

$$\tilde{I}_{k-1} = \sum_{j=1}^{k-1} \frac{Y_j}{\Delta} \int_{t_{j-1}}^{t_j} (1 - F(t_{k-1} - u)) du + \tilde{I}_0 (1 - F(t_{k-1})) \quad (28)$$

and  $\tilde{S}_{k-1}$  satisfies Eq (13).

**Remark 1** Better approximations for  $\mu_k$  are also available through higher order Taylor expansions for  $\tilde{S}_k(u)$  and  $\tilde{I}_k(u)$ , and with non-constant polynomial approximation for  $S'_j(u)$  in the observational window, while satisfying Eq (14), for all  $j = 1, 2, \dots, k-1$ .

#### 2.2.5 Identifiability

We use again Expression (17) to prove that the rate of infection  $\beta$  and the observed fraction  $p$  are identifiable.

**Theorem 2** Set

$$U_k = \int_{t_{k-1}}^{t_k} N^{-1} \tilde{S}_k(u) \tilde{I}_k(u) du \quad (29)$$

$$V_k = \int_{t_{k-1}}^{t_k} \tilde{I}_k(u) du. \quad (30)$$

If the vector  $(U_1, U_2, \dots, U_m)$  and  $(V_1, V_2, \dots, V_m)$  are linearly independent, then  $\beta$  and  $p$  are identifiable.

The proof of Theorem 2 is found in the appendix.

**Remark 2** *It follows from Theorem 2 that  $\beta$  and  $p$  are not identifiable from early outbreak data. Indeed, early in the outbreak,  $\tilde{S}_k(u) \approx N$ , so that the vectors  $(U_1, \dots, U_k)$  and  $(V_1, \dots, V_k)$  are essentially co-linear.*

### 2.3 Numerical parameter estimation

Metropolis-Hastings algorithm, a Markov chain Monte Carlo (MCMC) technique [44], is implemented in python programming language to numerically estimate the posterior distribution of the infection rate  $\beta$  and the fraction  $p$  of observed infected individuals for each country. First, the parameter  $\Theta = (\beta, p)$  is mapped into  $\tilde{\Theta} = (\xi, \eta)$  applying the transformation  $\xi = \log(\beta)$  and  $\eta = \log(p/(1-p))$ . So that, we generate a Markov chain sequence  $\{\tilde{\Theta}_m\}$  from the proposal bivariate normal distribution  $q(\cdot | \tilde{\Theta}_m) = N(\tilde{\Theta}_m, \Sigma)$ , with vector mean  $\tilde{\Theta}_m$  and covariance  $\Sigma$ , the diagonal matrix with entries 0.001 and 0.01.

In the MCMC implementation, we use Eq (23) to calculate the logarithm of the likelihood function,  $l(\tilde{\Theta}_m)$ , where  $\mu_k$  is numerically computed by implementing the equations from Lemma 1 with parameter value  $\Theta_m$ . The algorithm was iterated 80000 times with burn-in period of 10000 and initial value  $\Theta_0 = (0.5, 0.5)$ , with  $R_0 = 0$ ,  $\Delta = 1$ , and  $r = 25$ , for all countries. While the initial infected individuals,  $I_0$ , was set to the first incidence cases reported in the time series of each country.

## 3 Results

### 3.1 Analysis of COVID-19 incidence data

We apply our Bayesian analysis method to estimate the infection rate and the fraction of under-reporting incidence cases of SARS-CoV-2 in various American Countries: the United States of America (USA), Brazil, Mexico, Argentina, Chile, Colombia, Peru, and Panama. We modeled the time to recovery as the convolution of the lognormal distribution (mean=5.2, sdlog=0.662) with the Weibull distribution (mean=5, sd=1.9), which yields a distribution with recovery mean time of 10 days and standard deviation of 4 days [45, 46]. We refer the interested reader to [47] for a detailed description of relevant disease progression parameters of SARS-CoV-2 infection.

The time series of daily number of incidence cases for each country,  $\{Y_k\}$ , were obtained from WHO reports and set from the first confirmed positive case to November 10, 2020. To reduce the impact of reporting weekly reporting patterns, e.g., fewer cases are reported over the weekend, we apply a moving average of seven days to the raw incidence counts before execute the algorithm as described in Subsection 2.3. The assumption of constant infection rate does not hold, as each country implemented various mitigation and control strategies, from national lockdown orders to closing of public meeting places. Therefore, we decided to estimate the infection rate after mitigation were imposed [48]. In the algorithm, this corresponds to initialize  $k$  from Eq (23) at this intervention day accordingly to Table 1. However, the entire time series of incidence data were used to estimate the number of susceptible and infected individuals over time since the estimates for  $\tilde{S}_{k-1}$  and  $\tilde{I}_{k-1}$  do not depend directly on  $\beta$  nor  $p$ , see Eqs (13) and (28), while they encode the force of infection, dependency on  $\beta$  and  $p$ , in Eqs (26) and (27).

Table 1 summarizes the estimated values for the infectious transmission rate,  $\beta$ , and the fraction of reported cases,  $p$ , for each country, while Fig 1 and Fig 2 show their estimated posterior distributions. In the table, the parameter values correspond to their median estimated values and the interval values are the 95% confidence level to their

true values, i.e., the left and right end points of each interval coincide to the 0.025 and 0.975 percentiles of the resulted histograms, rounded to their nearest 100th values.

**Table 1. Parameter Median Values and Confidence Interval Estimations**

Country	$\beta$	95% CI ( $\beta$ )	$p$	95% CI ( $p$ )	First Case	Intervention
USA	0.117	[0.112, 0.121]	0.170	[0.124, 0.288]	January 20	March 22
Brazil	0.130	[0.126, 0.135]	0.073	[0.065, 0.083]	February 26	March 24
Mexico	0.127	[0.122, 0.132]	0.025	[0.021, 0.030]	February 28	March 23
Argentina	0.124	[0.120, 0.128]	0.089	[0.075, 0.112]	March 03	March 19
Chile	0.128	[0.123, 0.133]	0.082	[0.073, 0.096]	March 03	March 24
Colombia	0.123	[0.119, 0.127]	0.083	[0.069, 0.107]	March 06	March 25
Peru	0.135	[0.130, 0.140]	0.069	[0.063, 0.078]	March 07	March 16
Panama	0.116	[0.112, 0.121]	0.147	[0.116, 0.204]	March 10	March 24

In Table 1, from the estimated confidence intervals for  $\beta$ , the infectious transmission rate range from 0.112 to 0.140 among all countries. Being Panama and USA the countries with the smallest infection rate, whose median values are 0.116 and 0.117, respectively. While Peru accounts for the highest infection rate, whose median rate is 0.135. It is followed by Brazil whose infection median rate is 0.130.

Additionally, in Table 1, from the estimated confidence intervals for  $p$ , the fraction of reported incidence cases range from 0.021 to 0.288 among all countries. Being USA the country with the biggest fraction of reported incidence cases, accounting for 0.170 in median value. While Mexico have the smallest fraction of reported cases whose median value is 0.025. Interestingly, from Table 1, Fig 1, and Fig 2, Brazil, Mexico, Chile, and Peru are not observing more than 90% of their everyday infected individuals, while USA and Panama are observing 70–80% of the everyday infections.

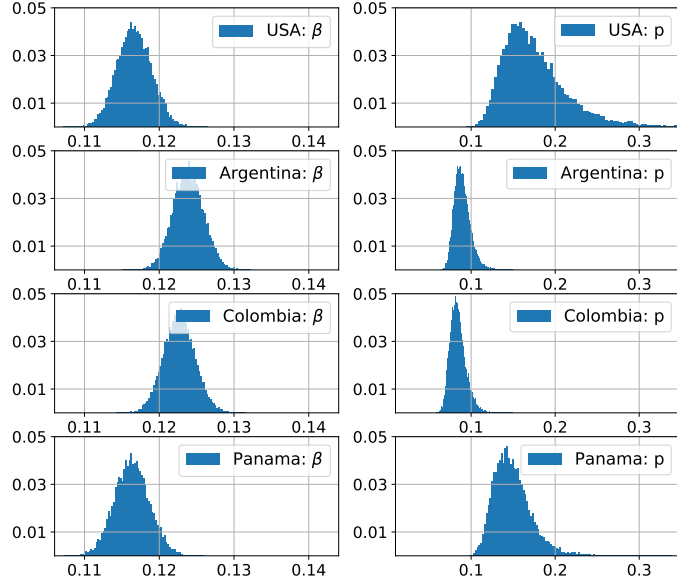


**Fig 1.** Histogram of the parameter values  $\beta$  (left) and  $p$  (right) resulting from the Bayes Analysis implementation for American countries that are observing more than 10% of all country infections.

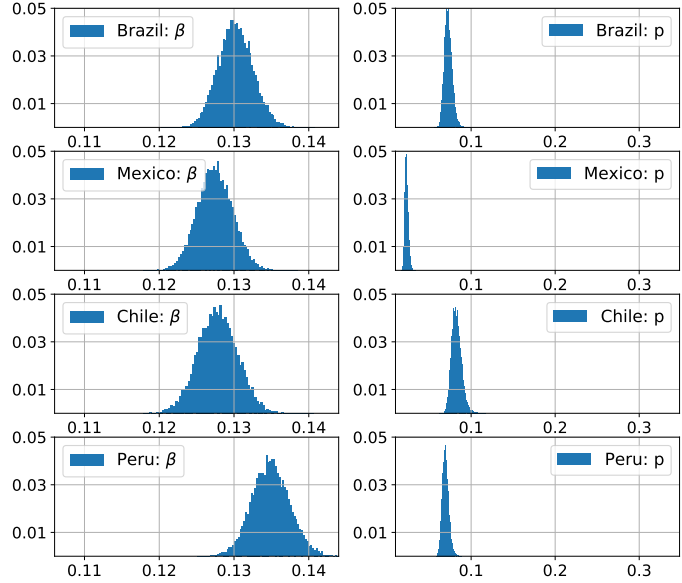


**Fig 2.** Histogram of the parameter values  $\beta$  (left) and  $p$  (right) resulting from the Bayes Analysis implementation for American countries that are observing less than 10% of all country infections.

Fig 1 and Fig 2 show the histograms for  $\beta$  and  $p$  values resulting from the MCMC implementation. In both figures, the estimated parameter values for  $\beta$  tend to be symmetrically distributed toward the mean values for all countries, ranging from about 0.110 to 0.142. While the  $p$  histograms for USA, Argentina, Colombia, and Panama skewed right lightly, whose values range from 0.06 to 0.3. However, the  $p$  histograms for Brazil, Mexico, Chile, and Peru exhibit a tight bell-shape, whose values range from 0.02 to 0.1.

### 3.2 Approximation of the COVID-19 data

We now proceed to describe the application of the method to estimate the conditional expectation of newly incidence counts with confidence bounds. The model is implemented using the equations provided in Lemma 1, with  $\beta$  and  $p$  median values from Table 1, for each American country. The predicted bounds for the numerical approximation of the expected daily incidence cases,  $\mu_k$ , are also computed using the negative binomial distribution assumption, Eq (19), with parameter  $r = 25$ . The lower and upper predicted bounds are set to value at the 2.5% and 97.5% of the generated distribution with parameters  $r/(r + \mu_k)$  and  $r$ , for each  $k = 1, 2, \dots, n$ , where  $n$  is the total number of observed days, starting from the day that the first no-zero case is reported till November 10, 2020.

Figs 3–10 show the resulted numerical approximations for the expected daily incidence counts and their predicted bounds, together with the WHO reported daily incidence cases for each country. The expected approximation values are plotted with red lines, the upper and lower predicted bounds are plotted with blue lines, while all the expected newly incidence values predicted by the model lie in the blue-shadow area,

with predicted probability of 95%. In all the figures, the raw incidence data lie within the confidence bounds as the epidemics evolves, resulting the model predictions properly to estimate the progression of reported daily incidence cases for these countries.

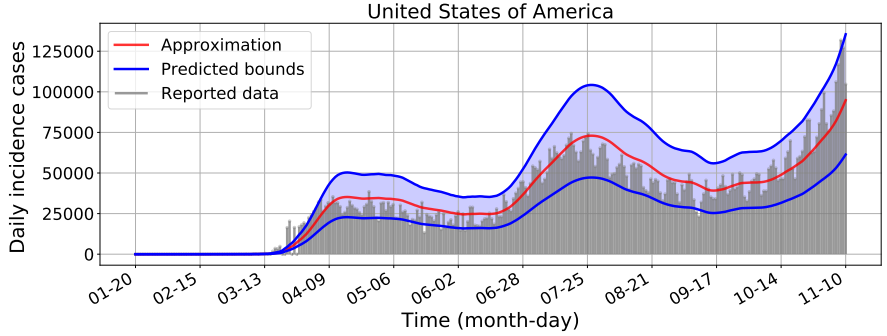


**Fig 3.** Daily incidence cases in the United States of America, from January 20 to November 10, 2020: newly cases reported from WHO (grey-bars), approximation of the conditional expectation (red-line), and 95% predicted bounds (blue-lines). Using the estimated infection rate  $\beta = 0.117$  and fraction of reported cases  $p = 0.170$ . Initial infected individuals  $I_0 = 5$ , population size  $N = 331,002,651$ , and observed days  $n = 296$ .

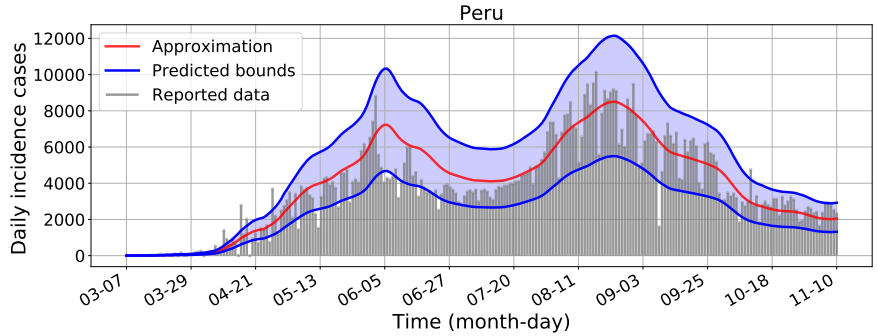


**Fig 4.** Daily incidence cases in Peru, from March 07 to November 10, 2020: newly cases reported from WHO (grey-bars), approximation of the conditional expectation (red-line), and 95% predicted bounds (blue-lines). Using the estimated infection rate  $\beta = 0.136$  and fraction of reported cases  $p = 0.064$ . Initial infected individuals  $I_0 = 10$ , population size  $N = 32,971,854$ , and observed days  $n = 249$ .

Additionally, Fig 3 shows that USA had three main report risings: early April, late June, and early October, which maintain that rising beyond November. Fig 4 shows that Peru registered two maximum incidences counts: first week of June and September, respectively. Its daily reported cases are now decreasing. Fig 5 shows that Chile registered a maximum incidence count by meddle of June. Now, it exhibits a decreasing trend in its reported incidence data. Figs 6, 7, 8, 9, and 10 show that Brazil, Mexico, Colombia, Argentina, and Panama have similar qualitative behaviours in their evolving incidence reported cases, where the counts increase early in the outbreak, achieve a maximum, and slowly decrease or sustain the epidemics. In all the figures, the model tracks the complex transmission trajectories of the evolving epidemic for each country.

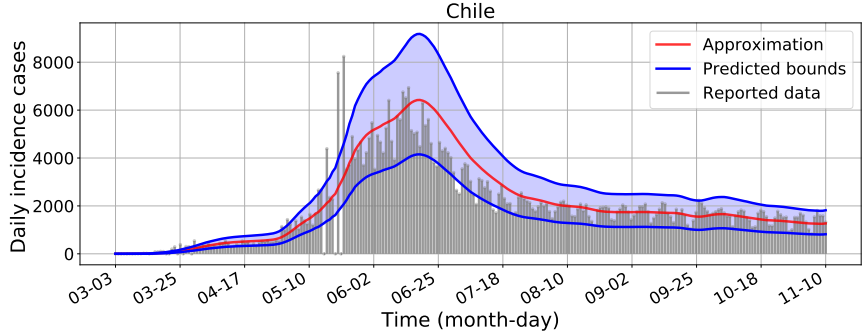


**Fig 5.** Daily incidence cases in Chile from March 03 to November 30, 2020: newly cases reported from WHO (grey-bars), approximation of the conditional expectation (red-line), and 95% predicted bounds (blue-lines). Using the estimated infection rate  $\beta = 0.127$  and fraction of reported cases  $p = 0.074$ . Initial infected individuals  $I_0 = 5$ , population size  $N = 45,195,774$  and observed days  $n = 253$ .

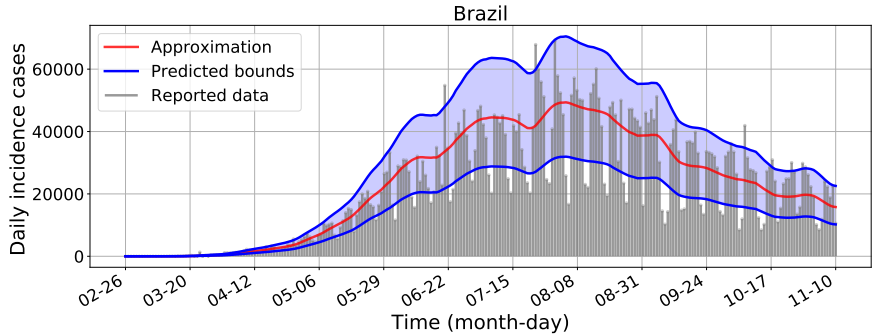


**Fig 6.** Daily incidence cases in Brazil, from February 26 to November 10, 2020: newly cases reported from WHO (grey-bars), approximation of the conditional expectation (red-line), and 95% predicted bounds (blue-lines). Using the estimated infection rate  $\beta = 0.130$  and fraction of reported cases  $p = 0.073$ . Initial infected individuals,  $I_0 = 5$ , population size  $N = 212,559,417$ , and observed days  $n = 259$ .

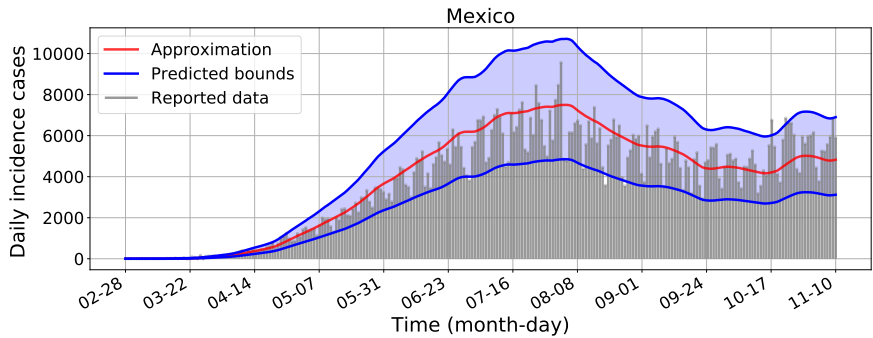


**Fig 7.** Daily incidence cases in Mexico, from February 28 to November 10, 2020: newly cases reported from WHO (grey-bars), approximation of the conditional expectation (red-line), and 95% predicted bounds (blue-lines). Using the estimated infection rate  $\beta = 0.127$  and fraction of reported cases  $p = 0.025$ . Initial infected individuals,  $I_0 = 6$ , population size  $N = 128,932,753$ , and observed days  $n = 257$ .

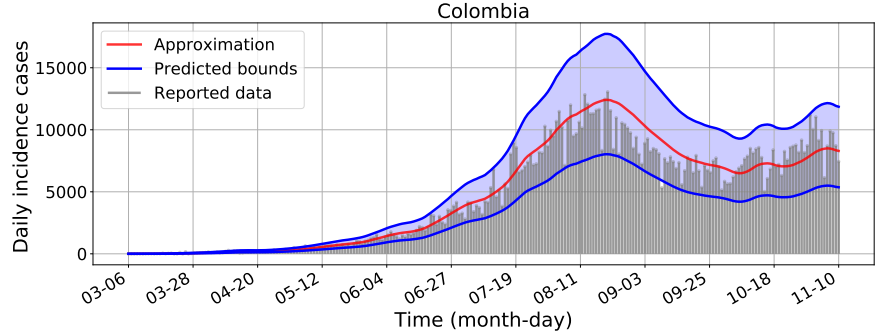


**Fig 8.** Daily incidence cases in Colombia, from March 06 to November 10, 2020: newly cases reported from WHO (grey-bars), approximation of the conditional expectation (red-line), and 95% predicted bounds (blue-lines). Using the estimated infection rate  $\beta = 0.123$  and fraction of reported cases  $p = 0.074$ . Initial infected individuals  $I_0 = 5$ , population size  $N = 50,882,891$ , and observed days  $n = 250$ .

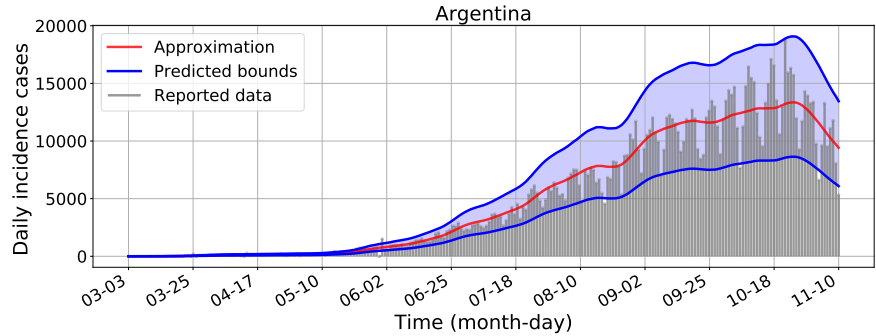


**Fig 9.** Daily incidence cases in Argentina, from March 03 to October 30, 2020: newly cases reported from WHO (grey-bars), approximation of the conditional expectation (red-line), and 95% predicted bounds (blue-lines). Using the estimated infection rate  $\beta = 0.123$  and fraction of reported cases  $p = 0.095$ . Initial infected individuals  $I_0 = 5$ , population size  $N = 45,195,774$ , and observed days  $n = 253$ .

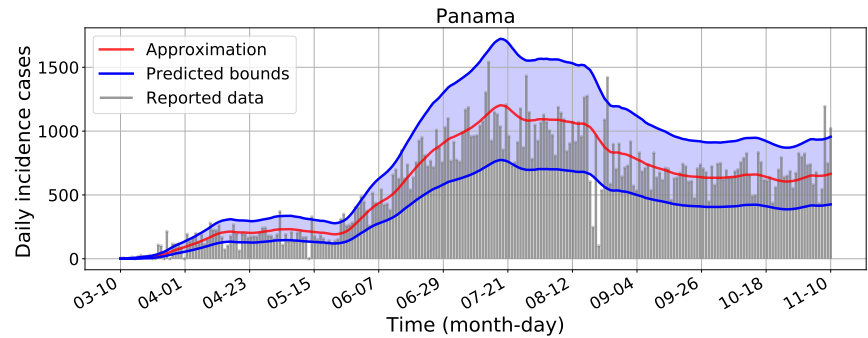


**Fig 10.** Daily incidence cases in Panama, from March 10 to November 10, 2020: newly cases reported from WHO (grey-bars), approximation of the conditional expectation (red-line), and 95% predicted bounds (blue-lines). Using the estimated infection rate  $\beta = 0.116$  and fraction of reported cases  $p = 0.147$ . Initial infected individuals  $I_0 = 5$ , population size  $N = 4,314,767$ , and observed days  $n = 246$ .

## 4 Discussion and Conclusion

Quantifying the lethality and infectiousness of emerging diseases such as the coronavirus disease (COVID-19) pandemic is challenging because of under-reporting of incidence cases [19, 27, 28, 49] that can be attributed to the presence of sub-clinical infections [20, 29], asymptomatic individuals [30, 31], and lack of systematic testing [17, 18]. In this paper, we present a novel approach to estimate the under-reporting from daily incidence data reports and apply that methodology to estimate the under-reporting of COVID-19 data in various American countries.

We first develop an extension of standard SIR epidemiological models to describe the temporal dynamics of the observed infectious diseases. The model extension shows that under-reported incidence cases lead to observe more susceptible and less infected and recovered individuals through an evolving epidemic. Additionally, fitting a SIR model type directly to raw incidence data will under-estimate the true infectious rate when neglecting under-reporting infectious cases, Subsection 2.2.2. Such results were also confirmed numerically by applying our methodology in the COVID-19 example, see the appendix.

Next, we formulate a stochastic model approach to approximate the expected number of newly infectious cases when we poses a time series of regularly incidence reports. This stochastic formulation allows to propose a Bayes analysis framework to estimate the infection rate and fraction of under-reporting. We prove mathematically that both parameters are identifiable, Subsection 2.2.5. Then, we propose a method to approximate the conditional expectation of newly infectious cases given the time series data, which can be easily implemented in programming languages, Subsection 2.2.4. We show the functionality of this method in Subsection 3.2.

Accordingly, from January 03 to November 10, 2020, assuming that in American countries, the COVID-19 epidemic evolves properly to a SIR model per day, with average recovered time of 10 days, and the time series of daily infection reports from WHO data follows a negative binomial distribution, as described in Section 2 and Section 3. Then, our analysis shows that the infectious rate in the United States of America, Brazil, Mexico, Argentina, Chile, Colombia, Peru, and Panama range from 0.112 to 0.140. Using the estimate of the reproductive number, Eq (4), it implies that the COVID-19 disease still spreading among these countries. The model analysis also reveals that consistently 70–90% of infected individuals were not observed in these American outbreaks. These results provide further evidence that COVID-19 carries a large fraction of under-reporting infectious cases [19, 30, 49].

The numerical simulations also show that the model can predict accurately the different qualitative behaviour of the evolving COVID-19 epidemic dynamics in the various American countries, with 95% confidence bounds. We performed sensitivity analysis on the parameter  $r$ , which results  $r = 25$  a reasonable value for the model predictions. Therefore, the presented stochastic model can be easily implemented and used to investigate the infectious transmission parameters and track complex epidemic trajectories.

## A Appendix

### A.1 Proof of existence and uniqueness of solutions of the generalized SIR model

To prove existence and uniqueness of solution of System (1,2,3), it is further assumed that the fraction of recovered individuals is defined through a probability distribution function,  $F : [0, \infty) \rightarrow [0, 1]$ , with the following properties.

**Property 1** *There exist an integrable function  $f : [0, \infty) \rightarrow [0, \infty)$  such that*

$$F(t) = \int_0^t f(u)du \quad \text{and} \quad \int_0^\infty f(u)du = 1,$$

*for all  $t \in [0, \infty)$ .*

**Property 2** *The average recovery time is finite, i.e.,*

$$\frac{1}{\gamma} = \int_0^\infty (1 - F(t))dt < \infty.$$

**Theorem 3** *Let  $U$  be an open set of  $[0, N] \times [0, N] \times [0, N] \times [0, \infty)$  and  $K$  a compact subset of  $U$  containing  $(S_0, I_0, R_0, t_0)$ , initial condition of System (1,2,3), with  $f(t)$  continuously differentiable with respect to  $t$ ,  $t \geq 0$  in  $U$ . Then there exist a unique solution of System (1,2,3) through the point  $(S_0, I_0, R_0)$  at  $t = 0$ , denoted  $X(S(t), I(t), R(t), t)$ , with  $X(S_0, I_0, R_0, 0) = (S_0, I_0, R_0)$ , for all  $t$  such that  $X(S(t), I(t), R(t), t) \in K$ .*

**Poof 1** *From Property 2, System (1,2,3) is well defined and it is equivalently to*

$$S'(t) = -\frac{\beta}{N}S(t)I(t) \quad (31)$$

$$I'(t) = \int_0^t f(t-u)S'(u)du - S'(t) - I_0f(t) \quad (32)$$

$$R'(t) = -\int_0^t f(t-u)S'(u)du + I_0f(t), \quad (33)$$

*which is obtained by taking the derivative with respect to  $t$  of Eqs (2) and (3) and using Property 1. Therefore, to prove existence and uniqueness of solutions of System (1,2,3) is equivalent to prove existence and uniqueness of solutions of System (31,32,33). It follows if the function  $G : U \rightarrow \mathbf{R}^3$  defined by*

$$G(S, I, R, t) = (S'(t), I'(t), R'(t)) \quad (34)$$

*is continuously differentiable in  $U$ , see for example [50, pp. 32]. Since  $\frac{\partial G}{\partial S}$ ,  $\frac{\partial G}{\partial I}$ ,  $\frac{\partial G}{\partial R}$ , and  $\frac{\partial G}{\partial t}$  exist and are continuous in  $U$ , then  $G$  is continuously differentiable in  $U$ . Therefore the solution of System (31,32,33) exist for the initial condition  $S_0, I_0, R_0$  and is unique in  $K$ .*

## A.2 Proof of Lemma 1

From Eq (9), for all  $0 \leq t \leq t_{k-1}$ ,

$$\begin{aligned} \tilde{I}(t) &= \sum_{j=1}^{k-1} \int_{t_{j-1}}^{t_j} \left( -\tilde{S}'(u) \right) (1 - F(t-u)) du \\ &\quad + \int_{t_{k-1}}^t \left( -\tilde{S}'(u) \right) (1 - F(t-u)) du + \tilde{I}_0(1 - F(t)). \end{aligned}$$

Therefore, for all  $t_{k-1} < t \leq t_k$ ,

$$\begin{aligned} \tilde{I}_k(t) &= \sum_{j=1}^{k-1} \int_{t_{j-1}}^{t_j} \left( -\tilde{S}'_j(u) \right) (1 - F(t-u)) du \\ &\quad + \int_{t_{k-1}}^t \left( -\tilde{S}'_k(u) \right) (1 - F(t-u)) du + \tilde{I}_0(1 - F(t)) \end{aligned}$$

where  $S'_j(u)$  satisfies Eq (8) for all  $u \in (t_{j-1}, t_j]$ ,  $j = 1, 2, \dots, k$ . Hence,

$$\tilde{I}_k(t_{k-1}) = \sum_{j=1}^{k-1} \int_{t_{j-1}}^{t_j} \left( -\tilde{S}'_j(u) \right) (1 - F(t_{k-1} - u)) du + \tilde{I}_0(1 - F(t_{k-1})),$$

and

$$\tilde{I}'_k(t_{k-1}) = - \sum_{j=1}^{k-1} \int_{t_{j-1}}^{t_j} \left( -\tilde{S}'_j(u) \right) f(t - u) du - \tilde{I}_0 f(t_{k-1}) - \tilde{S}'_k(t_{k-1}).$$

From these equations the rest of the proof follow easily by using the approximation hypothesis on each  $\tilde{S}'_j(u)$  and  $\tilde{S}'_j(u) \leq 0$ , for all  $j = 1, 2, \dots, k$ .

### A.3 Proof of Theorem 2

Set  $\alpha_1 = \beta/p$  and  $\alpha_2 = \beta(1-p)/p$ . Since

$$p = 1 - \frac{\alpha_2}{\alpha_1} \quad \text{and} \quad \beta = \alpha_1 - \alpha_2,$$

identifiability of  $\alpha_1$  and  $\alpha_2$  implies identifiability of  $\beta$  and  $p$ . We can estimate  $\alpha_1$  and  $\alpha_2$  by minimizing the sums of squares

$$\sum_{k=1}^m (Y_k - \alpha_1 U_k - \alpha_2 V_k)^2. \quad (35)$$

The two parameters are identifiable if and only if the vectors  $(U_1, \dots, U_m)$  and  $(V_1, \dots, V_m)$  are not co-linear.

### A.4 Under-estimation of the infectious rate

In Subsection 2.2.2, we prove that fitting a SIR model types directly to raw incidence data will under-estimate the true underlying infectious rate,  $\beta_1$ , when neglecting under-reporting infectious cases. Here, we apply our methodology to confirm this results, by fix  $p = 1$  and estimating  $\beta_1$  for all the studied American Countries, see Subsection 2.3 for the numerical model implementation. Table 2 summarizes the contrasting numerical parameter results, where  $\beta_p$  estimates coincide with the values from Table 1, while  $\beta_1$  refers to the model estimated results with fixed  $p = 1$ .

**Table 2. Parameter Median Values and Confidence Interval Estimations for the observed  $\beta_p$  and true underlying  $\beta_1$  rates.**

Country	$\beta_p$	95% CI ( $\beta_p$ )	$\beta_1$	95% CI ( $\beta_1$ )
USA	0.117	[0.112, 0.121]	0.110	[0.107, 0.112]
Brazil	0.130	[0.126, 0.135]	0.112	[0.109, 0.115]
Mexico	0.127	[0.122, 0.132]	0.112	[0.109, 0.116]
Argentina	0.124	[0.120, 0.128]	0.115	[0.112, 0.118]
Chile	0.128	[0.123, 0.133]	0.107	[0.105, 0.110]
Colombia	0.123	[0.119, 0.127]	0.113	[0.110, 0.116]
Peru	0.135	[0.130, 0.140]	0.112	[0.110, 0.115]
Panama	0.116	[0.112, 0.121]	0.107	[0.104, 0.110]

## References

1. Kermack WO, McKendrick AG. A contribution to the mathematical theory of epidemics. *Proceedings of the royal society of london Series A, Containing papers of a mathematical and physical character*. 1927;115(772):700–721.
2. Wilson EB, Worcester J. The law of mass action in epidemiology. *Proceedings of the National Academy of Sciences of the United States of America*. 1945;31(1):24.
3. Anderson RM, Anderson B, May RM. *Infectious diseases of humans: dynamics and control*. Oxford university press; 1992.
4. Brauer F, Castillo-Chavez C, Castillo-Chavez C. *Mathematical models in population biology and epidemiology*. vol. 2. Springer; 2012.
5. Diekmann O, Heesterbeek JAP. *Mathematical epidemiology of infectious diseases: model building, analysis and interpretation*. vol. 5. John Wiley & Sons; 2000.
6. Chowell G, Hengartner NW, Castillo-Chavez C, Fenimore PW, Hyman JM. The basic reproductive number of Ebola and the effects of public health measures: the cases of Congo and Uganda. *Journal of theoretical biology*. 2004;229(1):119–126.
7. Chowell G, Rivas A, Hengartner N, Hyman J, Castillo-Chavez C. The role of spatial mixing in the spread of foot-and-mouth disease. *Preventive Veterinary Medicine*. 2006;73(4):297–314.
8. Chowell G, Ammon CE, Hengartner NW, Hyman JM. Estimating the reproduction number from the initial phase of the Spanish flu pandemic waves in Geneva, Switzerland. *Mathematical Biosciences & Engineering*. 2007;4(3):457.
9. CDC. Centers for Disease Control and Prevention; 2020. Available from: <https://www.cdc.gov>.
10. University JH. COVID-19 Data Repository by the Center for Systems Science and Engineering (CSSE) at Johns Hopkins University; 2020. Available from: <https://github.com/CSSEGISandData/COVID-19>.
11. PAHO. Pan American Health Organization; 2020. Available from: <https://www.paho.org/en>.
12. WHO. COVID-19 Global Data, Geneva: World Health Organization; 2020. Available from: <https://covid19.who.int/WHO-COVID-19-global-data.csv> [cited 10 November 2020].
13. Del Valle SY, McMahon BH, Asher J, Hatchett R, Lega JC, Brown HE, et al. Summary results of the 2014-2015 DARPA Chikungunya challenge. *BMC infectious diseases*. 2018;18(1):245.
14. Lai CC, Liu YH, Wang CY, Wang YH, Hsueh SC, Yen MY, et al. Asymptomatic carrier state, acute respiratory disease, and pneumonia due to severe acute respiratory syndrome coronavirus 2 (SARSCoV-2): Facts and myths. *Journal of Microbiology, Immunology and Infection*. 2020;;
15. Kalajdzievska D, Li MY. Modeling the effects of carriers on transmission dynamics of infectious diseases. *Mathematical Biosciences & Engineering*. 2011;8(3):711.

16. Duffy MR, Chen TH, Hancock WT, Powers AM, Kool JL, Lanciotti RS, et al. Zika virus outbreak on Yap Island, federated states of Micronesia. *New England Journal of Medicine*. 2009;360(24):2536–2543.
17. Doll M, Pryor R, Mackey D, Doern C, Bryson A, Bailey P, et al. Utility of Re-testing for Diagnosis of SARS-CoV-2/COVID-19 in Hospitalized Patients: Impact of the Interval between Tests. *Infection Control & Hospital Epidemiology*. 2020; p. 1–6.
18. Esbin MN, Whitney ON, Chong S, Maurer A, Darzacq X, Tjian R. Overcoming the bottleneck to widespread testing: A rapid review of nucleic acid testing approaches for COVID-19 detection. *RNA*. 2020; p. rna–076232.
19. Li R, Pei S, Chen B, Song Y, Zhang T, Yang W, et al. Substantial undocumented infection facilitates the rapid dissemination of novel coronavirus (SARS-CoV2). *Science*. 2020;.
20. Team TNCPERE. The epidemiological characteristics of an outbreak of 2019 novel coronavirus disease (COVID-19) – China. *China CDC Weekly*. 2020;2(8):113–122.
21. Furuya-Kanamori L, Cox M, Milinovich GJ, Magalhaes RJS, Mackay IM, Yakob L. Heterogeneous and dynamic prevalence of asymptomatic influenza virus infections. *Emerging infectious diseases*. 2016;22(6):1052.
22. Reed C, Angulo FJ, Swerdlow DL, Lipsitch M, Meltzer MI, Jernigan D, et al. Estimates of the prevalence of pandemic (H1N1) 2009, United States, April–July 2009. *Emerging infectious diseases*. 2009;15(12):2004.
23. Shutt DP, Manore CA, Pankavich S, Porter AT, Del Valle SY. Estimating the reproductive number, total outbreak size, and reporting rates for Zika epidemics in South and Central America. *Epidemics*. 2017;21:63–79.
24. Hyman JM, Li J, Stanley EA. The differential infectivity and staged progression models for the transmission of HIV. *Mathematical biosciences*. 1999;155(2):77–109.
25. Romero-Severson EO, Hengartner N, Meadors G, Ke R. Decline in global COVID-19 transmission. *medRxiv*. 2020;doi:10.1101/2020.04.18.20070771.
26. Lopman B, Simmons K, Gambhir M, Vinjé J, Parashar U. Epidemiologic implications of asymptomatic reinfection: a mathematical modeling study of norovirus. *American journal of epidemiology*. 2014;179(4):507–512.
27. Ke R, Sanche S, Romero-Severson E, Hengartner N. Fast spread of COVID-19 in Europe and the US suggests the necessity of early, strong and comprehensive interventions; 2020. Available from: <https://doi.org/10.1101/2020.04.04.20050427>.
28. Read MC. EID: High contagiousness and rapid spread of severe acute respiratory syndrome coronavirus 2. *Emerg Infect Dis*. 2020;26.
29. Y B, L Y, T W, Tian F and CL Jih D Y and. Presumed asymptomatic carrier transmission of COVID-19. *J Am Med Assoc*. 2020;323(14):1406–1407.
30. Bar-On YM, Sender R, Flamholz AI, Phillips R, Milo R. A quantitative compendium of COVID-19 epidemiology. *arXiv preprint arXiv:200601283*. 2020;.

31. Rothe C, Schunk M, Sothmann P, Bretzel G, Froeschl G, Wallrauch C, et al. Transmission of 2019-nCoV infection from an asymptomatic contact in Germany. *New England Journal of Medicine*. 2020;382(10):970–971.
32. Bettencourt LM, Ribeiro RM. Real time bayesian estimation of the epidemic potential of emerging infectious diseases. *PLoS One*. 2008;3(5).
33. WHO. COVID-19 Explorer. Geneva: World Health Organization; 2020. Available from: <https://worldhealthorg.shinyapps.io/covid/> [cited 10 November 2020].
34. Hethcote HW, Tudor DW. Integral equation models for endemic infectious diseases. *Journal of mathematical biology*. 1980;9(1):37–47.
35. Murray J. *Mathematical Biology*, 2nd edition. Berlin: Springer-Verlag; 1993.
36. Heesterbeek JAP. A brief history of  $R_0$  and a recipe for its calculation. *Acta Biotheoretica*. 2002;50:189–204. doi:10.1023/A:1016599411804.
37. D FRSP, A AJLM. L. A problem in age-distribution. *The London, Edinburgh, and Dublin Philosophical Magazine and Journal of Science*. 1911;21(124):435–438.
38. Heesterbeek J, Dietz K. The concept of Ro in epidemic theory. *Statistica Neerlandica*. 1996;50(1):89–110.
39. Heffernan JM, Smith RJ, Wahl LM. Perspectives on the basic reproductive ratio. *Journal of the Royal Society Interface*. 2005;2(4):281–293.
40. Weiss HH. The SIR model and the foundations of public health. *Materials matemáticas*. 2013; p. 0001–17.
41. Team WER. Ebola virus disease in West Africa—the first 9 months of the epidemic and forward projections. *New England Journal of Medicine*. 2014;371(16):1481–1495.
42. Wang Z. One mixed negative binomial distribution with application. *Journal of Statistical Planning and Inference*. 2011;141(3):1153–1160.
43. Shmueli G, Minka TP, Kadane JB, Borle S, Boatwright P. A useful distribution for fitting discrete data: revival of the Conway–Maxwell–Poisson distribution. *Journal of the Royal Statistical Society: Series C (Applied Statistics)*. 2005;54(1):127–142.
44. Makowski D, Wallach D, Tremblay M. Using a Bayesian approach to parameter estimation; comparison of the GLUE and MCMC methods. *Agronomie*. 2002;22(2):191–203.
45. Ferretti L, Wymant C, Kendall M, Zhao L, Nurtay A, Abeler-Dörner L, et al. Quantifying SARS-CoV-2 transmission suggests epidemic control with digital contact tracing. *Science*. 2020;.
46. Li Q, Guan X, Wu P, Wang X, Zhou L, Tong Y, et al. Early transmission dynamics in Wuhan, China, of novel coronavirus–infected pneumonia. *New England Journal of Medicine*. 2020;.
47. Bar-On YM, Sender R, Flamholz AI, Phillips R, Milo R. A quantitative compendium of COVID-19 epidemiology; 2020.

48. Wikipedia. COVID-19 pandemic lockdowns; 2020. Available from: [https://en.wikipedia.org/wiki/COVID-19\\_pandemic\\_lockdowns](https://en.wikipedia.org/wiki/COVID-19_pandemic_lockdowns) [cited 10 November 2020].
49. Liu Z, Magal P, Seydi O, Webb G. Understanding unreported cases in the COVID-19 epidemic outbreak in Wuhan, China, and the importance of major public health interventions. *Biology*. 2020;9(3):50.
50. Wiggins S. Introduction to applied nonlinear dynamical systems and chaos. vol. 2. Springer Science & Business Media; 2003.